



Published in final edited form as:

Cornea. 2014 March ; 33(3): 280–287. doi:10.1097/ICO.000000000000050.

Predicting Trans-epithelial Phototherapeutic Keratectomy Outcomes Using Fourier-Domain Optical Coherence Tomography

Catherine Cleary, MD¹, Yan Li, PhD¹, Maolong Tang, PhD¹, Nehal Samy El Gendy, MD^{1,2}, and David Huang, MD, PhD¹

¹Center for Ophthalmic Optics and Lasers (www.COOLLab.net), Doheny Eye Institute and Department of Ophthalmology, Keck School of Medicine of the University of Southern California, Los Angeles, CA, USA

²Department of Ophthalmology, Kaser Al Aini School of medicine, Cairo University, Cairo, Egypt

Abstract

Purpose—To use Fourier-domain optical coherence tomography (FD-OCT) to predict trans-epithelial phototherapeutic keratectomy (TE-PTK) outcomes.

Methods—Prospective case series. Subjects with anterior stromal corneal opacities underwent excimer laser PTK combined with PRK using the VISX S4 excimer laser (AMO, Inc., Santa Ana, CA). Pre- and postoperative FD-OCT images were used to develop a simulation algorithm to predict treatment outcomes.

Main Outcome Measures—Pre- and postoperative uncorrected distance visual acuity (UDVA) and corrected distance visual acuity (CDVA). Postoperative corneal thickness and manifest refraction spherical equivalent (MRSE) were analyzed using multivariate linear regression.

Results—Nine eyes of 8 patients were treated. Nominal ablation depth was 75 – 177 μm centrally and 62 – 185 μm peripherally. Measured PTK ablation depths were 20% higher centrally and 26% higher peripherally, compared to laser settings. Postoperatively, mean UDVA was 20/41 (range 20/25 – 20/80) compared to 20/103 (range 20/60 – 20/400) preoperatively. Mean CDVA was 20/29 (range 20/15 – 20/60) compared to 20/45 (range 20/30 – 20/80) preoperatively. MRSE was $+1.38 \pm 2.37$ D compared to -2.59 ± 2.83 D (mean \pm SD). Mean astigmatism magnitude was 1.14 ± 0.83 D compared to 1.40 ± 1.18 D preoperatively. Postoperative MRSE correlated strongly with ablation settings, central and peripheral epithelial thickness ($r=0.99$, $p<0.00001$). Central island remained difficult to predict and limited visual outcomes in some cases.

Conclusion—OCT measurements of opacity depth and 3D ablation simulation provide valuable guidance PTK planning. Post-PTK refraction may be predicted with a regression formula which uses OCT epithelial thickness measurements. Laser ablation rates described in this study only apply to the VisX laser.

Correspondence to: David Huang, MD, PhD, Casey Eye Institute, 3375 SW Terwilliger Blvd, Portland, OR 97239, davidhuang@alum.mit.edu.

Proprietary interests: David Huang, Yan Li and Maolong Tang have significant financial interests in Optovue, Inc. (Fremont, CA, USA), a company that may have a commercial interest in the results of this research and technology. These potential conflicts of interest have been reviewed and managed by Oregon Health and Science University. Other author has no proprietary interest in the topic of this manuscript.

Keywords

optical coherence tomography; Fourier-domain optical coherence tomography; PTK; image-guided surgery; corneal opacity; corneal dystrophy; corneal scar

Introduction

Phototherapeutic keratectomy (PTK) is an important treatment for eyes with superficial corneal opacification or irregularity.¹⁻⁶ Trans-epithelial PTK (TE-PTK) has an advantage in comparison to PTK following epithelial removal, because the corneal epithelium serves as a masking agent, facilitating smoothing of anterior stromal irregularities.⁷

Until recently, the standard method to estimate required ablation depth in PTK was the slitlamp appearance of the depth of pathology, which lacks the precision to provide predictable results. Also, variable postoperative hyperopic shift can make refractive outcomes following PTK highly unpredictable. A method whereby planning PTK could be optimized in order to allow sufficient removal of corneal stromal opacities without inducing excessive hyperopic shift and corneal thinning, is needed.

Fourier-domain optical coherence tomography (FD-OCT)^{8,9} of the anterior segment can provide precise measurements both of the depth of corneal opacities,¹⁰⁻¹³ and of corneal epithelial thickness.¹⁴ The aim of this study was to develop a method where FD-OCT could be used to improve the predictability of TE-PTK outcomes.

Methods

Ethical approval for this study was granted by the Institutional Review Board of the University of Southern California Health Sciences Campus.

Subjects

Subjects with superficial corneal scars or dystrophies suitable for transepithelial PTK treatment were recruited from the cornea clinic at Doheny Eye Institute. Each subject gave informed consent both for surgery and for participation in this research study. Exclusion criteria included cases where adequate removal of opacity would leave less than 250 μm of residual stroma; nodular opacities superficial to Bowman's membrane, as in such cases mechanical peeling may leave a more regular surface than transepithelial ablation; and active corneal inflammation or infections.

Pre- and postoperative examinations

Demographic data and details of subjects' ophthalmic history were obtained from medical records. All patients underwent a full ophthalmic examination both pre- and postoperatively, including slitlamp examination, measurement of uncorrected and corrected distance visual acuity (UDVA and CDVA), and manifest refraction (MR). The pre- and postoperative manifest refractive spherical equivalent (MRSE) and astigmatism magnitude were calculated for each patient. Corneal topography and assessment of the irregularity index (for the central 3 mm of the cornea) was performed using Orbscan II (Bausch & Lomb, Inc., Rochester, New York, U.S.A.)

Optical Coherence Tomography

Corneal OCT images were obtained with a Fourier-domain OCT (RTVue-CAM by Optovue Inc., Fremont, California, U.S.A.) in all cases. The system works at 840 nm wavelength and

has a scan speed of 26,000 axial scans per second and depth resolution of 5 μm (full-width-half-maximum) in tissue. The wide-angle (corneal long) adaptor lens used in this study provides 6 mm long scan width and a transverse resolution of 15 μm (focused spot size). The RTVue-CAM was calibrated after system installation, and the calibration was verified weekly with the validation procedure recommended by the manufacturer.

“Pachymetry” and “CL-3D Cornea” scans were acquired preoperatively and 3 months after the surgery. The “Pachymetry” scan pattern consisted of 8 spoke-like arranged meridional scans (1024 axial scans per 6-mm long meridional scan) acquired in 0.3 seconds. “CL-3D Cornea” was a 3-dimensional (3D) scan pattern composed of 101 line scans (512 axial scans in each cross-sectional line scan). It covers a 6 \times 6 mm scan area and is acquired in 2 seconds. Both scan patterns were centered at the pupil center.

Pre- and post-operative corneal, epithelial and stromal thicknesses were obtained from OCT “Pachymetry” images in all subjects. All thickness measurements were made along the optical axis (parallel to the corneal vertex flare and the optical axis of the OCT system). We chose to measure parallel to the optical axis because the optical axis is also the axis of the excimer laser beam and thus facilitates subsequent calculations of ablation depth. All OCT measurements were obtained by one person (Y.L.).

The central corneal thickness was provided automatically by RTVue software and was the average of central 2 mm diameter zone (Version 4.0). We measured the peripheral corneal thickness at 4 peripheral locations (temporal, nasal, superior and inferior locations 2.5 mm away from the pupil center) with a computer caliper tool, and calculated a mean peripheral corneal thickness. The central epithelial thickness (CET) was measured inside the central 1.0 mm diameter area. The peripheral epithelial thickness (PET) was measured on both sides 2.5 mm from the corneal vertex. Values of PET from vertical and horizontal meridional images of the “Pachymetry” scan were averaged. In images where the epithelial thickness was highly variable, the average of measurements taken from at least 2 points of peak thickness and 2 points of low thickness, was used. The central and peripheral stromal thicknesses were calculated by subtracting epithelial thickness from corneal thickness at central and peripheral locations, respectively.

Opacity depth inside the central 6 mm optical zone was measured preoperatively using the computer caliper tool in all subjects. For purposes of laser ablation planning the measurement of each opacity at its deepest point was used.

Phototherapeutic keratectomy

TE-PTK was performed in all cases by the same surgeon (DH). After the instillation of topical anaesthetic drops (proparacaine hydrochloride 0.5%), the 3:00 and 9:00 positions at the limbus were marked with a surgical marking pen at the slitlamp. Following sterile preparation and draping, a lid speculum was placed, and the eye was centered under the VISX S4 excimer laser (AMO, Inc., Santa Ana, CA). Patient-specific K-readings were used when programming the VISX. The pulse rate of the laser ablations was 10 Hz. The patient was instructed to fixate on an internal fixation light, the head position was adjusted to align the limbal orientation marks, and the pre-programmed ablations were delivered.

To plan laser ablations, we used a nomogram which combined PTK with PRK with the aim of reducing postoperative refractive error.¹⁵ Our aim was to ensure the combined ablation was deep enough to completely remove the epithelium and also remove most of the superficial stromal opacity within the optical zone. Prophylactic anti-central island ablation was added in cases which required deep PTK ablation or had a pre-existing central steep zone. For each subject, the amount of refractive ablation required was estimated based on

the preoperative MR and the surgeon's estimation of the amount of hyperopic shift likely to be induced by the PTK treatment. In some cases hyperopic ablations were added to neutralize some of the induced hyperopia from the PTK ablations. The PTK-induced hyperopic shift was estimated using Munnerlyn's formula, for example an ablation depth of 12 microns will produce a refractive change of 1 Diopter when the optical zone diameter is 6mm.

The ablation sequence began with an optional prophylactic anti-central island ablation using PTK (piston-shaped) mode with an ablation diameter of 3.5–4.5 mm with a 1.4–1.8 mm transition zone. The depth of the anti-central island ablation was generally 15% of the PTK ablation but was adjusted by the surgeon depending on whether the central region on preoperative topography was steeper or flatter than the periphery. Next transepithelial ablation in plano PTK mode of 6.5 mm diameter with 0.5 mm transition zone width was performed. The depth of transepithelial ablation was at least equal to the maximum epithelial thickness in the central 6 mm optical zone, measured by OCT. This was followed by further PTK and PRK depending on the subjects' preoperative refractive error, opacity depth and corneal thickness. PRK options included myopia, hyperopia, myopic astigmatism, or hyperopic astigmatism corrections as needed. The refractive ablations all used a 6-mm diameter optical zone. Treatment zone diameter was 6 mm for myopic and 9 mm for hyperopic ablations. A thin film of saline was applied to smooth the corneal surface before starting the first ablation. In some cases, the final 20 μm of PTK ablation was performed with the use of 0.5% carboxymethylcellulose as masking agent,¹⁶ if stromal irregularity was noted by the surgeon near the end of the PTK ablation.

In all cases following laser treatment, 0.02% mitomycin-C was applied to the central cornea for 2 minutes on a 7-mm diameter cellulose sponge. The ocular surface was irrigated with BSS for 2 minutes, and a soft contact lens applied. Prednisolone acetate 1%, Ketorolac trimethamine 0.5%, and gatifloxacin 0.3% eye drops were instilled. Prednisolone acetate 1% and gatifloxacin 0.3% eye drops were used qid for 1 week postoperatively. Prednisolone 1% was then used bid for 1 month and od for 1 month.

Ablation efficiency

A custom algorithm developed with MATLAB 7.0 (The MathWorks, Inc., Natick, MA, USA) was used to calculate the ablation map, ablation efficiency, central island effect, and perform the surgical simulation.

The nominal laser ablation map of each eye under treatment was calculated according to the laser settings, including PTK (plano), refractive, and anti-central island components. Based on surgical experience (but no formal study), we reduced the amount of ablation performed with the masking agent by 50% in the ablation map calculation to account for the effect of the masking fluid. The central and peripheral nominal ablation amounts were obtained from the nominal ablation map.

The actual laser ablation depth (TE-PTK) was calculated as the difference between the preoperative corneal thickness and the postoperative corneal stromal thickness, on OCT (i.e. the difference between the TE-PTK depth and the central epithelial thickness is the stromal thickness ablated by the TE-PTK ablation). Ablation efficiency was evaluated by comparing the TE-PTK depth to the nominal laser ablation settings. A custom algorithm was used to calculate the numerical ablation maps using parabolic ablation assumptions. The central ablation depth calculated by the custom algorithm was verified to match the central ablation depth printed on the VISX report.

Linear regression between the nominal laser ablation setting and the actual laser ablation depth was performed to determine the ablation efficiencies, both centrally and peripherally. The intercept of the linear regression line was set to zero (Figure 1).

Computerized PTK simulation

Details of the methods of computerised PTK simulation used to simulate the tissue removal during surgery are given in Appendix 1.

Statistical analysis

Descriptive and analytical statistics including *t*-tests and multi-variable linear regression were performed using Excel 2010 software (Microsoft Corp., Redmond, WA, USA).

Visual acuity was converted from Snellen notation to log minimum angle of resolution (logMAR) for statistical analysis¹⁵. In cases where PTK retreatment was performed, we used the final visual outcome following the second treatment to calculate visual improvement. A paired *t*-test was used to compare pre- and post-operative visual acuities. A formula to correlate the spherical equivalent refractive outcome with pre-operative corneal measurements and the PTK ablation depth was developed using multivariable linear regression. The spherical equivalent refractive change before and after the surgery was related to the relative thickness of central and peripheral epithelial thickness (CET and PET, respectively) measures by OCT, in addition to the PTK depth and refractive ablation settings.

Two variables “TE-PTK depth – CET” and “CET – PET” were involved in the multi-variable linear regression because: Firstly, the difference between the PTK depth and central epithelial thickness may be related to the post-surgery epithelial remodeling process. Secondly, the central – peripheral difference in epithelial thickness may affect the refractive outcome (hyperopic or myopic shifts). Linear regression analysis was used to compare the actual versus calculated spherical equivalent refractive outcomes to assess the multi-variable formula (Figure 2). Spectacle plane laser refractive settings are reported in Table 1. These were converted to the corneal plane before performing the refractive linear regression.

Results

Nine eyes from 6 males and 2 females were treated (Table 1, Table 2), 5 with traumatic corneal scars, 2 from one patient with Reis-Buckler dystrophy (Figure 3) and 2 eyes from 2 patients with granular dystrophy (Figure 4). The mean age was 52 ± 20 (mean \pm SD, range 21 to 72) years. All cases received treatment in the TE-PTK mode (wide uniform beam). Myopic astigmatism ablation was used in all cases except Case 3. Hyperopic astigmatism ablation was used in Cases 3, 5, and 6 (Table 1). Case 3 had anti-central island ablation during the primary treatment. Case 4 underwent PTK retreatment to remove residual scar. Case 5 had PTK retreatment to remove steep central island secondary to the primary PTK treatment (Figure 5).

Visual acuity and refractive outcomes

Pre- and postoperative visual acuities, MRSE, mean astigmatism magnitude and mean irregularity index are reported in Table 3. The mean improvement in UDVA was 4.0 ± 3.5 lines ($p < 0.01$), and in CDVA was 2.0 ± 1.9 lines ($p < 0.05$). One eye in the study (Case 7, see Table 1) lost 2 lines of CDVA, going from 20/40 to 20/60, this was due to progression of cataract. Mean change in MRSE was $+3.44 \pm 2.69D$.

Laser ablation efficiency

The central and peripheral nominal and actual laser ablation depths are listed in Table 4. The laser ablation efficiency determined by linear regression analysis was 120% (R = 0.973) in the center and 126% (R = 0.974) at the periphery (Figure 1).

Actual versus calculated refractive outcomes

A formula to correlate the spherical equivalent refractive outcome with the OCT epithelial measurements and surgical settings was obtained by least-square multivariate linear regression (Equation 1):

$$SED = -0.29 + 0.141 * (TE - PTK \text{ depth} - CET) - 0.159 * (CET - PET) \quad (\text{Equation 1})$$

Where TE-PTK depth was the transepithelial PTK ablation depth, CET was the central epithelial thickness, and PET was the peripheral epithelial thickness. The units of the intercept coefficient are Diopters (D). The units of the slope coefficients are D/ μm . The dependent variable in the equation, the spherical equivalent deviation (SED) was defined as follows:

SED = surgically induced spherical equivalent refractive change – (spherical equivalent laser setting)

The refractive change was the surgically achieved MRSE change (post-operative MRSE – preoperative MRSE). The spherical equivalent laser setting adds the spherical equivalent of both myopic and hyperopic ablations.

The mean central – periphery epithelial thickness difference (CET-PET) in our case series was $2 \pm 6 \mu\text{m}$, (range –7 to 12 μm). Using the $-0.159(\text{CET-PET})$ term in Equation 1, this corresponded to a range of +1.07 to –1.91 D in refractive effect from epithelial thickness variation.

In this data set, the formula was highly predictive of refractive outcomes, (Pearson's correlation coefficient $r = 0.99$). Both PTK setting (PTK depth-CET, $p < 0.0001$) and corneal epithelial mask power (CET-PET; $p < 0.05$) were significant factors. The p value of the slope coefficient 0.141 for (PTK depth – CET) was < 0.00001 . The p value of the slope coefficient -0.159 for (CET-PET) was < 0.05 . The p value of the intercept -0.29 was 0.359. The p value of the whole model was < 0.00001 . The slope of the MRSE prediction was 1.00 [95% CI 0.88 to 1.12]. A linear relationship between the actual refractive changes and the calculated refractive change was verified (Figure 2). The formula was used to build a nomogram to enable prediction of refractive outcomes in future cases.

Case Reports on case numbers 5 and 6 are detailed in Appendix 2.

Discussion

Mori *et al* were the first to develop an OCT-based PTK simulation algorithm using three-dimensional volume data from a 1310 nm high-speed swept-source OCT system, and reported good outcomes using this algorithm to guide PTK treatment.¹⁸ This small pilot study provides a model based on 840nm FD- OCT measurements which may improve the predictability of refractive outcomes following transepithelial PTK.

Using precise measurements obtained with OCT, we calibrated the VISX PTK ablation depth and discovered the actual central ablation was 20% deeper than the nominal settings. This is highly effective for opacity removal, but means more stroma is removed, and more hyperopic shift is induced, than necessary. We found a 20% reduction in the nominal

ablation settings improves the control and predictability of PTK ablation depth. For example, if the desired central ablation depth is 120 μm , the programmed ablation depth should be set at 100 μm to compensate for the higher than nominal ablation efficiency.

FD-OCT allows accurate measurement of corneal epithelial thickness. We found that differences in preoperative CET and PET may be associated with refractive shifts after TE-PTK. Reinstein *et al* have reported on epithelial thickness changes following LASIK surgery,¹⁷ and we acknowledge that in the future it may potentially be important to study the effect of postoperative epithelial thickness changes in our model. It has also been reported that the refractive effect of TE-PTK can be purely astigmatic depending on the epithelial thickness profile,³⁶ and it may be that measurements of epithelial thickness could be used to identify cases that do not fall into a myopic or hyperopic pattern. It is also possible that the laser ablation rate might be different for epithelium than for stroma, which could have an impact when combining transepithelial and stromal PTK.³⁵ A mean hyperopic shift of +3D (range +1.0 to +5.25 D) has been reported following PTK.²² This phenomenon is highly variable and unpredictable, and is most pronounced at 1 month postoperatively with regression occurring up to 1 year.^{4,20–24} Postulated causes of hyperopic shift include central cornea flattening, epithelial thickness modulation, and increases in peripheral corneal thickness.^{17,25,26,28} We hypothesize that part of the post-PTK refractive shift could be due to masking by the epithelium during transepithelial ablation.²⁶ For example, if the corneal epithelium is thinner centrally than peripherally, the piston-shaped PTK laser ablation will remove more stromal tissue in the center than at the periphery. This effect is similar to myopic refractive laser correction. Alternatively, if the epithelium is thicker centrally than peripherally, the piston-shaped PTK ablation will remove stromal tissue more at the periphery than in the center – similar to hyperopic laser correction. This hypothesis was confirmed by the negative coefficient (-0.159) of the CET-PET term in Equation 1. This regression formula could be used to predict post-PTK refractive outcomes by plugging in pre-operative OCT measurements (CET and PET) and surgical settings (PTK depth, refractive ablation setting). This is a new application of OCT which has not previously been described.

No automatic compensatory anti-central island ablation is provided in the VISX lasers for the PTK mode. For refractive ablations, this problem has been largely overcome by the use of compensatory anti-central island ablations.^{32–34} Although we developed our own anti-central island ablation method,^{27,29–31} the results were poorly predictable and the cases which underwent deep PTK ablation still developed significant central islands despite anti-central island ablations. We observed one case of vision-limiting steep central island after deep PTK ablation for Reis-Buckler dystrophy, which required a second PTK treatment. Steep central island was also observed in the fellow eye of the same patient, but retreatment was not indicated as the vision was satisfactory. The use of flying-spot lasers to perform PTK may help to avoid this problem.

Our study has some limitations. Firstly it was a small pilot study with only 9 eyes. We hope to conduct more studies with larger numbers to further improve our methods. Although we have succeeded in predicting the magnitude of hyperopic shift following PTK with greater accuracy, some hyperopic shift remains unavoidable, especially in cases where deep PTK ablations are required. Also, our PTK methodology was not successful in reducing cylinder magnitude. The cylindrical laser ablation setting was determined by topographic analysis and refraction, both of which measurements were prone to inaccuracy due to the high degree of irregular astigmatism in these cases. The OCT map may contain more precise information on corneal astigmatism, but we have not as yet succeeded in developing a reliable method to extract this data. Another limitation is that we used data from the 3 month postoperative visit¹⁷ to derive the prediction model for transepithelial PTK. Postoperative epithelial

changes may continue for longer periods of time, which may also influence the accuracy of the model.

In this study, both UCVA and CDVA were stable or improved in 88% of cases. This improvement in vision was due to reduction in both corneal opacity and irregularity. Although the topographic irregularity index was not significantly reduced, we hypothesise that the epithelial masking provided smoothing on a small scale not well measured by placido topography.^{17,25} Subepithelial smoothing can be seen on postoperative OCT images (Figure 5). One of the reasons corneal surface irregularity was not improved more was the unpredictable induction of steep central island, and flying spot lasers may produce better results by avoiding this problem.

In conclusion, we found that FD-OCT is useful in the refinement of PTK technique and may be useful in the future in planning individual cases.

Supplementary Material

Refer to Web version on PubMed Central for supplementary material.

Acknowledgments

Financial Support: NIH grant R01EY018184, research grant from Optovue, Inc., grant from Research to Prevent Blindness, Charles C. Manger III, MD Chair in Corneal Laser Surgery endowment

Dr Catherine Cleary is supported by a grant from the Irish College of Ophthalmologists.

References

1. Maloney RK, Thompson V, Ghiselli G, Durrie D, Waring GO 3rd, O'Connell M. A prospective multicenter trial of excimer laser phototherapeutic keratectomy for corneal vision loss. The Summit Phototherapeutic Keratectomy Study Group. *Am J Ophthalmol*. 1996; 122:149–160. [PubMed: 8694083]
2. Kozobolis VP, Siganos DS, Meladakis GS, Pallikaris IG. Excimer laser phototherapeutic keratectomy for corneal opacities and recurrent erosion. *J Refract Surg*. 1996; 12:S288–290. [PubMed: 8653512]
3. Orndahl M, Fagerholm P, Fitzsimmons T, Tengroth B. Treatment of corneal dystrophies with excimer laser. *Acta ophthalmologica*. 1994; 72:235–240. [PubMed: 8079631]
4. Rapuano CJ. Excimer laser phototherapeutic keratectomy: long-term results and practical considerations. *Cornea*. 1997; 16:151–157. [PubMed: 9071527]
5. Hersh PS, Spinak A, Garrana R, Mayers M. Phototherapeutic keratectomy: strategies and results in 12 eyes. *Refract Corneal Surg*. 1993; 9(2 Suppl):S90–95. [PubMed: 8499388]
6. Hersh PS, Burnstein Y, Carr J, Etwaru G, Mayers M. Excimer laser phototherapeutic keratectomy. Surgical strategies and clinical outcomes. *Ophthalmology*. 1996; 103:1210–1222. [PubMed: 8764789]
7. Muller LT, Candal EM, Epstein RJ, Dennis RF, Majmudar PA. Transepithelial phototherapeutic keratectomy/photorefractive keratectomy with adjunctive mitomycin-C for complicated LASIK flaps. *J Cataract Refract Surg*. 2005; 31:291–296. [PubMed: 15767148]
8. Huang D, Swanson EA, Lin CP, et al. Optical coherence tomography. *Science*. 1991; 254:1178–1181. [PubMed: 1957169]
9. Choma M, Sarunic M, Yang C, Izatt J. Sensitivity advantage of swept source and Fourier domain optical coherence tomography. *Optics express*. Sep 8.2003 11:2183–2189. [PubMed: 19466106]
10. Khurana RN, Li Y, Tang M, Lai MM, Huang D. High-speed optical coherence tomography of corneal opacities. *Ophthalmology*. 2007; 114:1278–1285. [PubMed: 17307254]

11. Vajzovic LM, Karp CL, Haft P, et al. Ultra high-resolution anterior segment optical coherence tomography in the evaluation of anterior corneal dystrophies and degenerations. *Ophthalmology*. 2011; 118:1291–1296. [PubMed: 21420175]
12. Ma JJ, Tseng SS, Yarascavitch BA. Anterior segment optical coherence tomography for transepithelial phototherapeutic keratectomy in central corneal stromal scarring. *Cornea*. 2009; 28:927–929. [PubMed: 19654520]
13. Song, J.; Huang, D., editors. *Corneal Opacities*. Thorofare, NJ: Slack; 2008. Steinert, RF.; Huang, D., editors. *Anterior Segment Optical Coherence Tomography*.
14. Wirbelauer C, Scholz C, Haberle H, Laqua H, Pham DT. Corneal optical coherence tomography before and after phototherapeutic keratectomy for recurrent epithelial erosions(2). *J Cataract Refract Surg*. 2002; 28:1629–1635. [PubMed: 12231324]
15. Zaidman GW, Hong A. Visual and refractive results of combined PTK/PRK in patients with corneal surface disease and refractive errors. *J Cataract Refract Surg*. 2006; 32:958–961. [PubMed: 16814053]
16. Kornmehl EW, Steinert RF, Puliafito CA. A comparative study of masking fluids for excimer laser phototherapeutic keratectomy. *Arch Ophthalmol*. 1991; 109:860–863. [PubMed: 2043076]
17. Reinstein DZ, Archer TJ, Gobbe M. Change in epithelial thickness profile 24 hours and longitudinally for 1 year after myopic LASIK: three-dimensional display with Artemis very high-frequency digital ultrasound. *J Refract Surg*. 2012; 28:195–201. [PubMed: 22301100]
18. Mori H, Miura M, Iwasaki T, et al. Three-dimensional optical coherence tomography-guided phototherapeutic keratectomy for granular corneal dystrophy. *Cornea*. 2009; 28:944–947. [PubMed: 19654514]
19. Reinstein DZ, Silverman RH, Trokel SL, Coleman DJ. Corneal pachymetric topography. *Ophthalmology*. 1994; 101:432–438. [PubMed: 8127563]
20. Amm M, Duncker GI. Refractive changes after phototherapeutic keratectomy. *J Cataract Refract Surg*. 1997; 23:839–844. [PubMed: 9292665]
21. Campos M, Nielsen S, Szerenyi K, Garbus JJ, McDonnell PJ. Clinical follow-up of phototherapeutic keratectomy for treatment of corneal opacities. *Am J Ophthalmol*. 1993; 115:433–440. [PubMed: 8470713]
22. Dogru M, Katakami C, Yamanaka A. Refractive changes after excimer laser phototherapeutic keratectomy. *J Cataract Refract Surg*. 2001; 27:686–692. [PubMed: 11377896]
23. Nassaralla BA, Garbus J, McDonnell PJ. Phototherapeutic keratectomy for granular and lattice corneal dystrophies at 1.5 to 4 years. *J Refract Surg*. 1996; 12:795–800. [PubMed: 8970027]
24. Gartry D, Kerr Muir M, Marshall J. Excimer laser treatment of corneal surface pathology: a laboratory and clinical study. *Br J Ophthalmol*. 1991; 75:258–269. [PubMed: 1817467]
25. Reinstein DZ, Archer TJ, Gobbe M, Silverman RH, Coleman DJ. Epithelial thickness after hyperopic LASIK: three-dimensional display with Artemis very high-frequency digital ultrasound. *J Refract Surg*. 2010; 26:555–564. [PubMed: 19928697]
26. Huang D, Tang M, Shekhar R. Mathematical model of corneal surface smoothing after laser refractive surgery. *Am J Ophthalmol*. 2003; 135:267–278. [PubMed: 12614741]
27. Forster W, Clemens S, Bruning, Magnago T, Elsner C, Krueger R. Steep central islands after myopic photorefractive keratectomy. *J Cataract Refract Surg*. 1998; 24:899–904. [PubMed: 9682107]
28. Dupps WJ Jr, Roberts C. Effect of acute biomechanical changes on corneal curvature after photokeratectomy. *J Refract Surg*. 2001; 17:658–669. [PubMed: 11758984]
29. Krueger RR, Saedy NF, McDonnell PJ. Clinical analysis of steep central islands after excimer laser photorefractive keratectomy. *Arch Ophthalmol*. 1996; 114:377–381. [PubMed: 8602772]
30. Cua IY, Pepose JS. Proper positioning of the plume evacuator in the VISX Star3 excimer laser minimizes central island formation in patients undergoing laser in situ keratomileusis. *J Refract Surg*. 2003; 19:309–315. [PubMed: 12777026]
31. Itoi M, Ryan R, Depaolis M, Aquavella JV. Clinical effect of blowing nitrogen gas across the cornea during photorefractive keratectomy. *J Refract Surg*. 1997; 13:69–73. [PubMed: 9049938]
32. Rachid MD, Yoo SH, Azar DT. Phototherapeutic keratectomy for decentration and central islands after photorefractive keratectomy. *Ophthalmology*. 2001; 108:545–552. [PubMed: 11237909]

33. Alio JL, Artola A, Rodriguez-Mier FA. Selective zonal ablations with excimer laser for correction of irregular astigmatism induced by refractive surgery. *Ophthalmology*. 2000; 107:662–673. [PubMed: 10768327]
34. Castillo A, Romero F, Martin-Valverde JA, Diaz-Valle D, Toledano N, Sayagues O. Management and treatment of central steep islands after excimer laser photorefractive keratectomy. *J Refract Surg*. 1996; 12:715–720. [PubMed: 8895128]
35. Seiler T, Kriegerowski M, Schnoy N, Bende T. Ablation rate of human corneal epithelium and Bowman's layer with the excimer laser (193 nm). *Refract Corneal Surg*. 1990; 6:99–102. [PubMed: 2248922]
36. Reinstein DZ, Archer TJ, Gobbe M. Refractive and topographic errors in topography-guided ablation produced by epithelial compensation predicted by three-dimensional Artemis very high-frequency digital ultrasound stromal and epithelial thickness mapping. *J Refract Surg*. 2012; 28:657–663. [PubMed: 22947295]

Ablation Efficiency

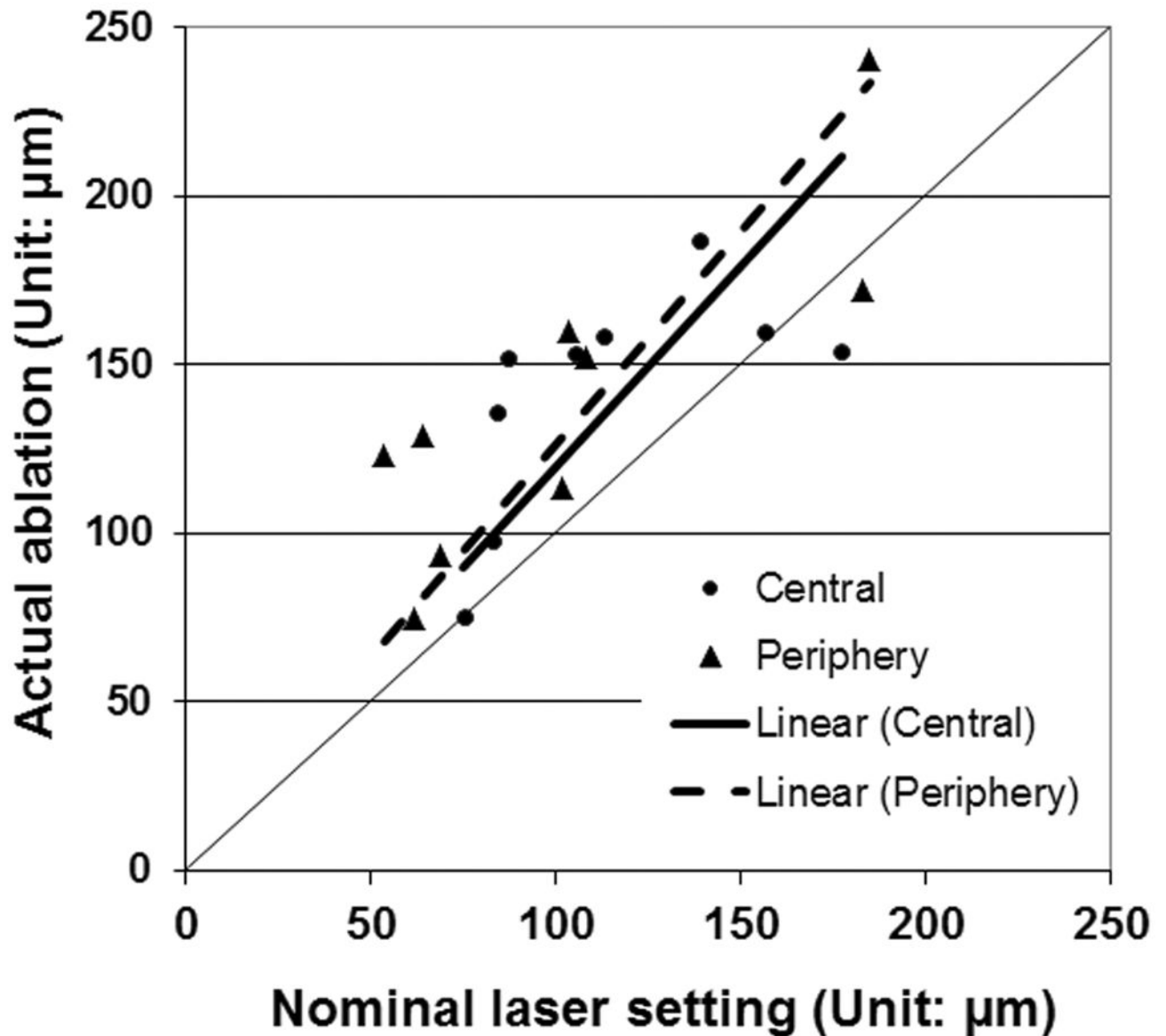


Figure 1.

Linear regression plots to evaluate the excimer laser ablation in the center and at the periphery. The thick solid line is the regression line for central ablation ($y=1.1957x$). The dashed line is the regression line for periphery ablation ($y=1.2628x$). The thin solid line is $y=x$. In cases where subjects had 2 PTK surgeries, data from the first surgery only is included in this graph.

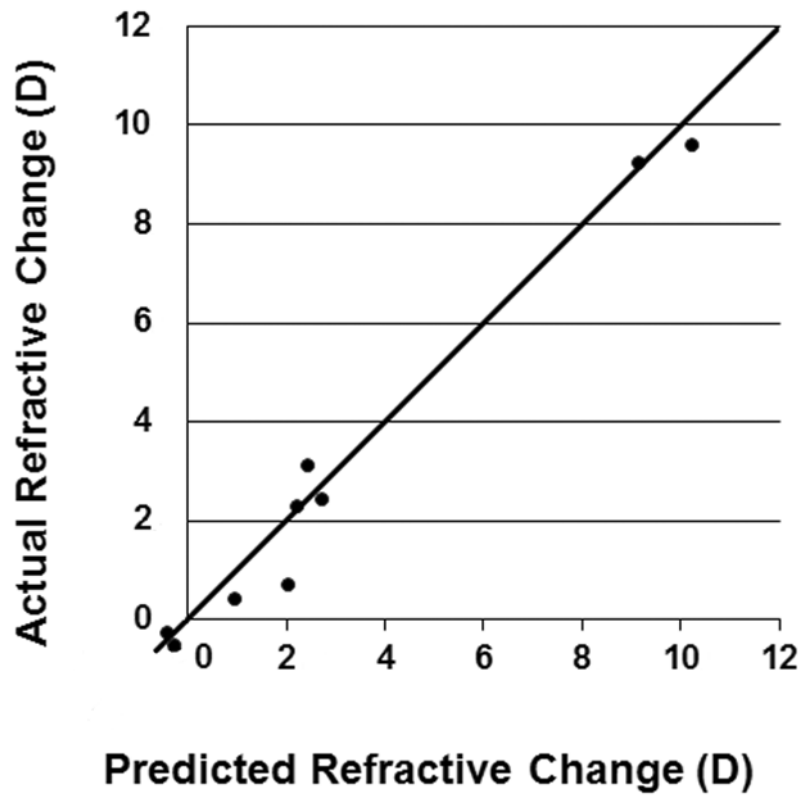


Figure 2. This graph illustrates the linear relationship between the calculated refractive change using the OCT-based equation and the actual refractive change following phototherapeutic keratectomy (PTK) for corneal scarring.

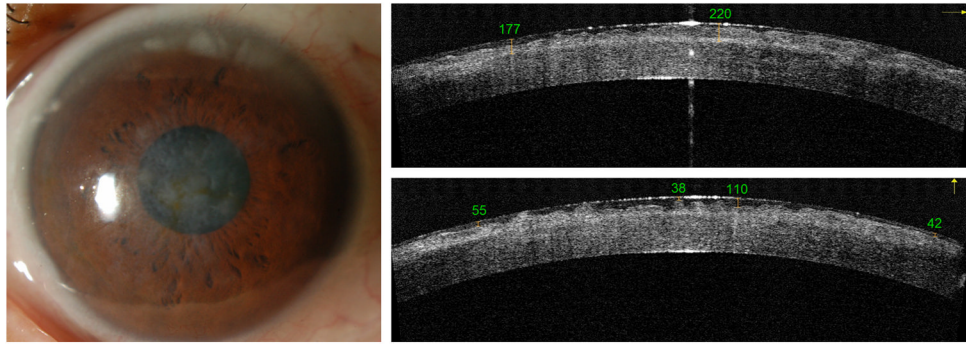


Figure 3. Preoperative clinical photograph (A) and FD-OCT images (B and C) in a case of Reis-Buckler dystrophy (Case 5). Irregular anterior stromal scarring and variable corneal epithelial thickness are visible on OCT imaging.

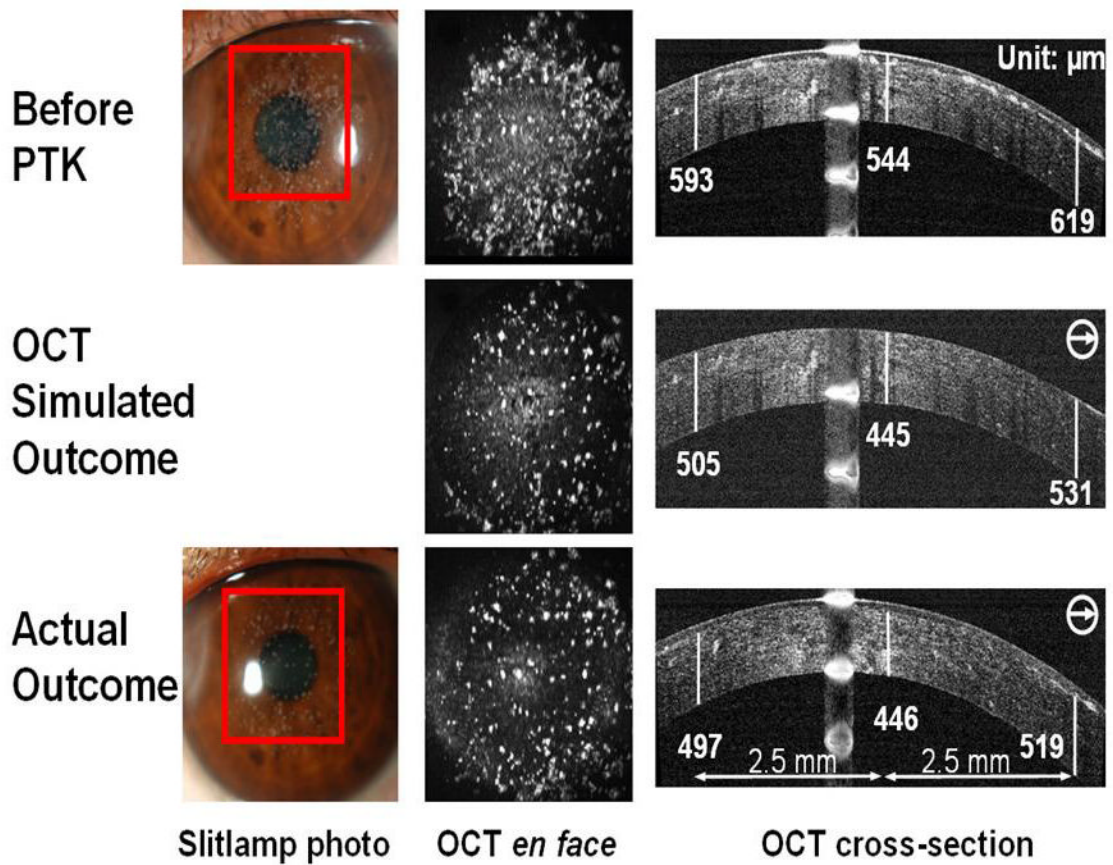


Figure 4.

This figure compares the preoperative, simulated outcome and actual post-PTK outcome in a case of granular dystrophy (Case 6). The OCT simulated outcome corresponds closely with the actual postoperative outcome. Subepithelial smoothing of anterior stromal irregularities was seen on postoperative OCT images (actual outcome).

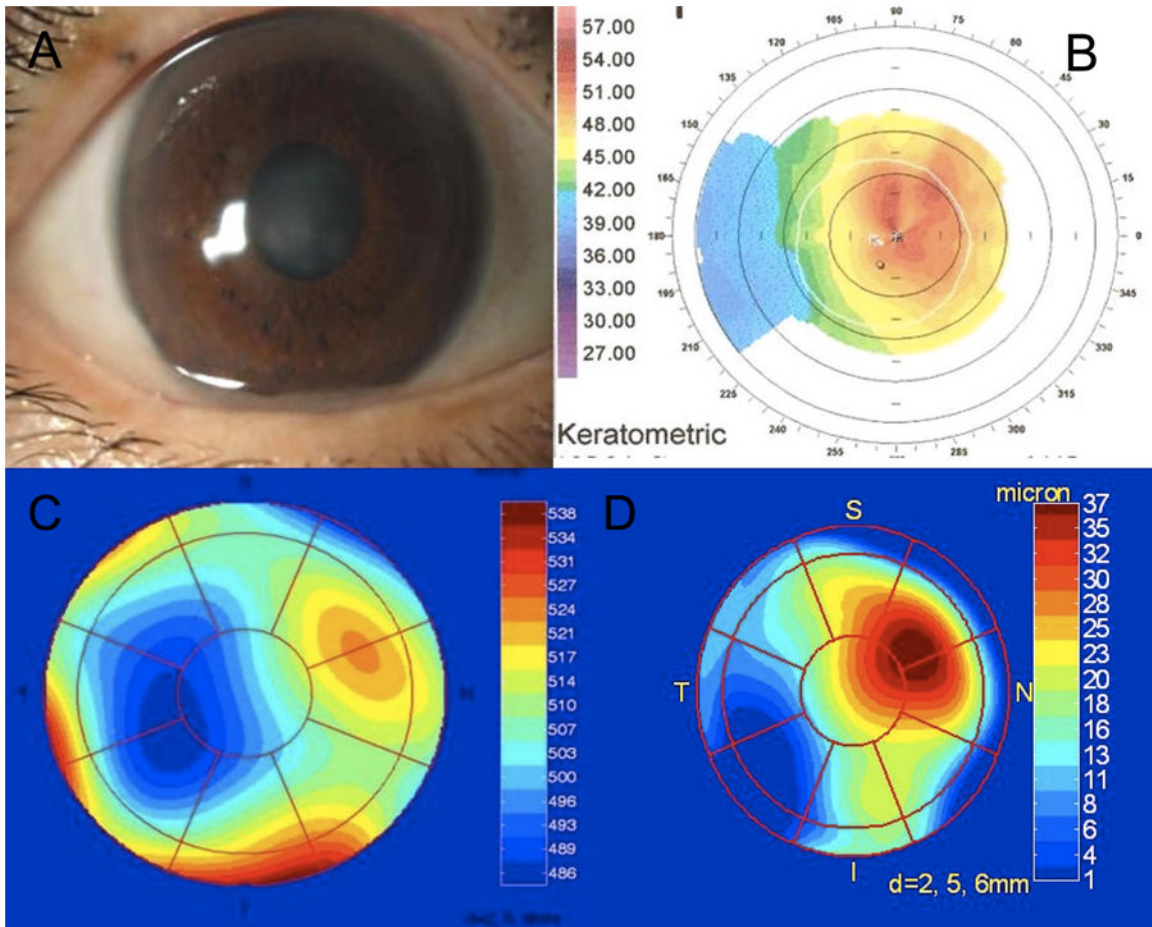


Figure 5. Case 5, three months postoperatively. Right eye CDVA is limited to 20/100, due to the presence of corneal haze (A), and a central island which was detected on the Orbscan axial power map (B). The central island was not directly visible on the OCT pachymetry map (C), however its presence was demonstrated by subtracting the best-fit underlying sphere to obtain a difference map (D). Based on the OCT difference map the central island was 37 μm in magnitude and deviated from the pupil center by 1 mm at 25 degrees (D).

Summary of Phototherapeutic Keratectomy Cases, including diagnosis, laser procedure type, and pre-and postoperative visual acuities and refractions.

Table 1

Case	Eye	Diagnosis	Laser Procedure Type	Preoperative CDVA	Postoperative CDVA	Preoperative Refraction	Postoperative Refraction (D)
1	OS	Scar	PTK/PRK(M &A)+MMC	20/40	20/15	-2.75/-1.25 × 178	+0.5/-0.5 × 160
2	OD	Scar	PTK/PRK(M&A)+MMC	20/30	20/30	-1.25/-1.5 × 101	-0.25/-0.5 × 132
3	OD	Granular dystrophy	PTK/PRK (H)+MMC	20/30	20/20	+2.0/-1.0 × 137	+2.25 DS
4	OD	Scar	PTK/PRK (M&A)+MMC	20/30	20/20	-8.5/-0.25 × 55	+0.75/-1.5 × 181*
5	OD	Reiss Buckler	PTK/PRK(M, H&A)+MMC	20/80	20/40	-1.25/-1.25 × 180	+6.5/-2.0 × 180*
5	OS	Reiss Buckler	PTK/PRK (M,&H&A)	20/80	20/40	-4.5 DS	+5.0/-1.75 × 180
6	OS	Granular dystrophy	PTK/PRK(M&A)	20/50	20/25	-0.75/-2.25 × 10	+3.0/-2.25 × 10
7	OD	Scar	PTK/PRK(M&A)+MMC	20/40	20/60	plano/-4.0 × 133	plano/-1.0 × 115
8	OD	Scar	PTK/PRK(M&A)+MMC	20/60	20/30	-1.5/-1.0 × 175	+1.75/-0.5 × 175

M= Myopic PRK ablation, H= Hyperopic PRK ablation, A= Astigmatic PRK ablation, MMC= Mitomycin-C.

* Final postoperative refraction following PTK retreatment.

Table 2

Summary of laser treatment settings and OCT measurements.

Case	Eye	Intended Laser Ablation Depth (µm)*	Retreatment Ablation Depth (µm)	Actual Central Ablation Depth (µm)	Simulated OCT Ablation Depth	Central Ablation Difference (%)	Peripheral Ablation Difference (%)	Central Island Height (µm)	Central Island (%)	Central Epithelial Thickness (CET, µm)	Peripheral Epithelial Thickness (PET, µm)	CET-PET (µm)
1	OS	94	NA	136	108.8	-61.9%	-131.7%	17.8	30.6%	63.5	49	14.5
2	OD	75	NA	75	97.1	0.0%	-19.6%	13.0	22.7%	61	59.5	1.5
3	OD	128	NA	153.5	136.0	-46.2%	-40.6%	-4.6	-4.6%	77.75	71.25	6.5
4	OD	174**	77	160	202.5	-2.3%	-11.2%	8.0	8.9%	56	56	0
5	OD	149**	43	187	180.0	-34.5	-30.1	7.6	5.9	76	44.35	31.75
5	OS	177	NA	154	229.3	13.0	6.1%	12.1	8.9%	66.5	48.5	18
6	OS	84	NA	98	107.4	-18.2	-36.1%	9.6	15.0%	55	61.75	-6.75
7	OD	87	NA	152	112.7	-74.7	-101.2%	-0.2	-0.4%	62	65	-3
8	OD	100	NA	158.5	146.1	-40.5	-55.0%	11.0	12.3%	85.5	50.75	34.75

* nominal laser setting

** ablation depth from primary treatment and retreatment were added

Table 3

Pre- and postoperative visual acuities, MRSE, mean astigmatism magnitude and mean irregularity index following OCT-guided transepithelial PTK.

	Preoperative	Postoperative	p
UDVA (logMAR)	0.71 ± 0.27	0.31 ± 0.16	<0.01
CDVA (logMAR)	0.36 ± 0.17	0.16 ± 0.19	<0.05
UDVA (Snellen)	20/103 (range 20/60 to 20/400)	20/41 (range 20/25 to 20/80)	<0.01
CDVA (Snellen)	20/45 (range 20/30 to 20/80)	20/29 (range 20/15 to 20/60)	<0.05
MRSE (D)	-2.59 ± 2.83 (range -8.625 to +2.25)	+1.38 ± 2.37 (range -0.625 to +4.75)	<0.01
Mean Astigmatism Magnitude (D)	1.40±1.18 (range 1.0 to 2.25)	1.14±0.83 (range 0.5 to 2.3)	ns
Mean irregularity index	4.20 ± 1.88 (range 1.7 to 7.9)	4.41±1.43 (range 2.5 to 7.9)	ns

Table 4

Differences measured by OCT between the preoperative central and peripheral mean epithelial thicknesses, the nominal and actual laser ablation depths, and laser ablation efficiency of the VISX laser in PTK mode.

	Center	Periphery	p
Mean epithelial thickness	60 ± 11 μm (range 55 to 78)	58 ± 9 μm (range 44–71)	ns
Mean nominal laser ablation depth	113 ± 36 μm (range 75 to 177)	103 ± 50 μm (range 62–183)	<0.05
Mean actual laser ablation depth	142 ± 34 μm (range 75 to 187)	140 ± 49 μm (range 62 to 185)	<0.05
Mean difference between nominal and actual laser ablation depths	28 ± 30 μm (range –23 to 65)	16 ± 20 μm (range –15 to 38)	ns
Laser ablation efficiency	120%	126%	<0.00001